256 Slice Multi-detector Computed Tomography Thoracic Aorta Computed Tomography Angiography: Improved Luminal Opacification Using a Patient-Specific Contrast Protocol and Caudocranial Scan Acquisition

Charbel Saade, PhD,† Fadi El-Merhi, MD, ABR,* Bassam El-Achkar, MD,* Racha Kerek, PhD,* Thomas J. Vogl, MD,‡ Gilbert Georges Maroun, MD,* Lamia Jamjoom, MD,§ Hussain Al-Mohiy,† and Lena Naffaa, MD**

Clinical Relevance Statement: Caudocranial scan direction and contrast injection timing based on measured patient vessel dynamics can significantly improve arterial and aneurysmal opacification and reduce both contrast and radiation dose in the assessment of thoracic aortic aneurysms (TAA) using helical thoracic computed tomography angiography (CTA).

Objectives: To investigate opacification of the thoracic aorta and TAA using a caudocranial scan direction and a patient-specific contrast protocol.

Materials and Methods: Thoracic aortic CTA was performed in 160 consecutive patients with suspected TAA using a 256-slice computed tomography scanner and a dual barrel contrast injector. Patients were subjected in equal numbers to one of two contrast protocols. Patient age and sex were equally distributed across both groups. Protocol A, the department's standard protocol, consisted of a craniocaudal scan direction with 100 mL of contrast, intravenously injected at a flow rate of 4.5 mL/s. Protocol B involved a caudocranial scan direction and a novel contrast formula based on patient cardiovascular dynamics, followed by 100 mL of saline at 4.5 mL/s. Each scan acquisition comprised of 120 kVp, 200 mA with modulation, temporal resolution 0.27 seconds, and pitch 0.889:1. The dose length product was measured between each protocol and data generated were compared using Mann-Whitney *U* nonparametric statistics. Receiver operating characteristic analysis, visual grading characteristic (VGC), and κ analyses were performed.

Results: Mean opacification in the thoracic aorta and aneurysm measured was 24 % and 55%, respectively. The mean contrast volume was significantly lower in protocol B (73 ± 10 mL) compared with A (100 ± 1 mL) (P<0.001). The contrast-to-noise ratio demonstrated significant differences between the protocols (protocol A, 18.2 ± 12.9; protocol B, 29.7 ± 0.61; P < 0.003). Mean effective dose in protocol B (2.6 ± 0.4 mSv) was reduced by 19% compared with A (3.2 ± 0.8 mSv) (P < 0.004). Aneurysmal detectability demonstrated significant increases by receiver operating characteristic and visual grading characteristic analysis for protocol B compared with A (P < 0.02), and reader agreement increased from poor to excellent.

Conclusions: Significant increase in the visualization of TAAs following a caudocranial scan direction during helical thoracic CTA can be achieved using low-contrast volume based on patient-specific contrast formula.

Key Words: 256 slice MDCT, thoracic aortic CTA, thoracic aortic aneurysms, patient specific contrast formula

(*J Comput Assist Tomogr* 2016;40: 964–970)

Thoracic computed tomography (CT) angiography (TCTA) has become a robust clinical tool for the diagnosis and exclusion thoracic aortic aneurysms (TAA).[1–3] This is mostly due to the high sensitivity and negative predictive value of the test.[3] Recent concerns about the radiation exposure of the patient led to the introduction of low-dose protocols for TCTA.[4] Currently, no system is in place to track a patient's lifetime cumulative dose from medical sources,[5,6] and questions have arisen regarding the possible threat to public health from the widespread use of CT and the efficacy of the test ordered.

The efficacy of TCTA and particularly its ability to quantify the entire luminal sac is completely reliant on effective contrast administration protocols.[7] Contrast media protocols should be designed to incorporate 4 key variables: anatomical coverage, scan time, time to peak (TTP) at the thoracic aorta (cardiovascular circulation), and contrast injection flow rate. Predetermined contrast volumes (CVs) (based on user experience) ranging from 15 to 150 mL and injection rates from 2 to 5 mL/s have been reported[8]; however, these studies did not use a holistic approach to contrast administration where the variables would change seamlessly to the changing patient, protocol, and contrast media injection rate. Therefore, resulting in limited translation into clinical practice,[9–11] due to complexities and end-user knowledge. Based on these changing variables, the aim of this TCTA study is to investigate the impact of patient-specific contrast administration protocols on TAA and visualization of the thoracic vasculature.

MATERIALS AND METHODS

Study Population

The institutional review board approved this study and written informed consent was waived because all studies were clinically indicated and patient data was evaluated anonymously. Between November 2012 and January 2014, 160 consecutive patients (mean age, 77 years; range, 55–99 years; 100 men, 60 women) were included in this study (Table 1). Patients were referred from the emergency department with suspected TAA after clinical assessment and determined by evaluating mediastinal widening on a chest x-ray.[12]

From the *Department of Diagnostic Radiology, American University of Beirut Medical Center, Beirut, Lebanon; †Department of Diagnostic Radiology, College of Applied Medical Sciences, King Khalid University, Abha, Saudi Arabia; ‡Johann Wolfgang Goethe-Universität Frankfurt, Frankfurt, Germany; and §Radiology Department, King AbdulAziz University Hospital, Jeddah, Saudi Arabia.

Received for publication December 4, 2015; accepted March 29, 2016.

Correspondence to: Charbel Saade, PhD, Department of Diagnostic Radiology, American University of Beirut Medical Center, PO Box: 11-0236 Riad El Solh, Beirut 1107 2020 Beirut, Lebanon (e-mail: info@mdct.com.au).

Disclosure: (1) The scientific guarantor of this publication is Charbel Saade. (2) The authors of this manuscript declare no relationships with any companies, whose products or services may be related to the subject matter of the article. (3) The authors state that this work has not received any funding. (4) One of the authors (C.S.) has significant statistical expertise. No complex statistical methods were necessary for this paper. (5) Institutional Review Board approval was obtained. (6) Written informed consent was not required for this study because we were performing a retrospective study between previous and current practice. Written informed consent was waived by the Institutional Review Board. (7) Approval from the institutional animal care committee was not required because it was human studies. (8) Some study subjects or cohorts have not been previously reported. (9) Methodology: retrospective, diagnostic or prognostic study, performed at one institution.

DOI: 10.1097/RCT.0000000000000456

TABLE 1. Patient Demographics

Parameter	Protocol A	Protocol B	*P*
Male	50	50	>0.05
Female	30	30	>0.05
Age, y	77 ± 11.2	73 ± 11.9	>0.05
Height, cm	171 ± 12	174 ± 9	>0.05
Weight, kg	78 ± 9	81 ± 9.2	>0.05
BMI, kg/m^2	25.6 ± 5.5	25.4 ± 6.2	>0.05

Data are mean ± standard deviation.
BMI indicates body mass index.

Thoracic CT Angiography Acquisition

All examinations were performed using a 256-slice multidetector computed tomography scanner (Philips iCT; Philips Healthcare, The Netherlands), and patients were positioned supine with arms above the head. Anterior-posterior scout scan was performed before the scan acquisition, with a scan range from the diaphragm (2 cm below the costophrenic angle) to the sternal notch (2 cm above the aortic arch). Shallow breath-holds, with a mouth open breathing technique were used to reduce hyperventilation and valsalva. For both protocols, the scanner, contrast, and reconstruction parameters are shown in Table 2.

Contrast Bolus Geometry

Bolus geometry is the pattern of enhancement within a region of interest (ROI) after intravascular injection of contrast material, plotted as opacity (HU) versus time. The 2 protocols used different bolus-tracking techniques. Protocol A used a dynamic bolus tracking where the ROI is plotted inside the lumen of the ascending aorta (annulus segment) with a fixed CV (100 mL). A trigger attenuation value threshold (100 HU) above the baseline was arbitrarily chosen with a delay of 5 seconds from reaching the threshold to the start of the computed tomography angiography (CTA) acquisition. The volume of contrast material was not tailored to the patient's body mass index,[13] but was based on current departmental work practice and in line with current literature.[14] Protocol B used the test bolus technique where the ROI is plotted within the thoracic aorta (at the diaphragmatic hiatus level) using a small amount of contrast material (10 mL) administered at the same rate as the main bolus and the TTP was measured. Both protocols used a 100-mL saline chaser injected at 4.5 mL/s.

Contrast Medium Administration

Contrast material and saline chaser were injected with an automated dual barrel power injector (Optivantage, Mallinckrodt, Cincinnati) via a 20G venous catheter in the right arm. For protocol B, the CV was calculated according to the empirically derived formula[15]:

$$CV = (ST + TTP - OVWP) \times FR$$

where ST is the scan time (seconds), TTP (seconds) is as described above, OVWP is the optimal venous washout phase (12 seconds), and FR is the flow rate (mL/s). ST differs for each patient based on the distance between the diaphragm and apices of the thorax. OVWP was fixed at 12 s,[16,17] because this value was arbitrary chosen because it is a constant in the mean total time it takes from the beginning of the injection at the antecubital fossa until the time it reaches the right atrium. This was therefore, substituted with saline to reduce the redundant contrast media in the venous system entering the right atrium during scan acquisition, that caused perivenous artefacts along the ascending aorta.

Image Assessment

Transaxial images were reconstructed with 0.625-mm slice thickness (0.5 mm increment) using a smoothing convolution kernel (field of view, 380 × 380 mm; image matrix, 512 × 512). Image quality assessment using a reporting workstation (IMPAX 6.3.1, AGFA) with grayscale standard display function-calibrated 3 megapixel monitor included attenuation measurements, receiver operating characteristic (ROC) methods for TAA detection and visual grading characteristic (VGC) techniques to evaluate contrast media filling within the aneurysm.

Attenuation Measurements

Mean vessel HU values were obtained from axial images using a circular ROI with the greatest diameter that would fit within the lumen and exclude the vessel wall and intramural thrombus. Arterial measurements were performed at 9 anatomical segments incorporating the surgical landing zones of the thoracic aorta.[18] Each measurement was taken by orthogonal cross-section from the sites listed below and shown in Figure 1:

- Ascending aorta: sinus of valsalva, sinotubular junction, body and distal segment;
- Arch of aorta: first segment (between innominate and left common carotid artery), second segment (between the left common carotid and left subclavian artery), and aortic isthmus;
- Descending aorta: proximally at the levels of the aortic valve and aortic hiatus.

Contrast-to-Noise Ratio Measurement

Contrast-to-noise ratio (CNR) analysis was calculated using a 3-mm thick transaxial image. The ROI was drawn as large as the vessel lumen diameter carefully avoiding calcified and/or soft

TABLE 2. Scanner, Contrast, and Reconstruction Parameters

	Protocol A	Protocol B
Scanner parameters		
kVp	120	120
Rotation time, s	0.4	0.4
Pitch	0.889:1	0.889:1
mA (modulation)	200	200
Direction/range	Craniocaudal	Caudocranial
Contrast bolus geometry		
Bolus tracking	Bolus triggering	Test bolus
Region of interest	Ascending aorta	Descending aorta
Contrast parameters		
Contrast volume, mL	100	Formula
Flow rate, mL/s	4.5	4.5
Saline volume, mL	100	100
Flow rate, mL/s	4.5	4.5
Reconstruction parameters		
Reconstruction type	FBP	FBP
Slice thickness, mm	256 × 0.625	256 × 0.625
Reconstruction interval, mm	0.5	0.5
Field of view, mm	350 × 350	350 × 350
Window with and level	420:65	420:65

FBP indicates filtered back projection.

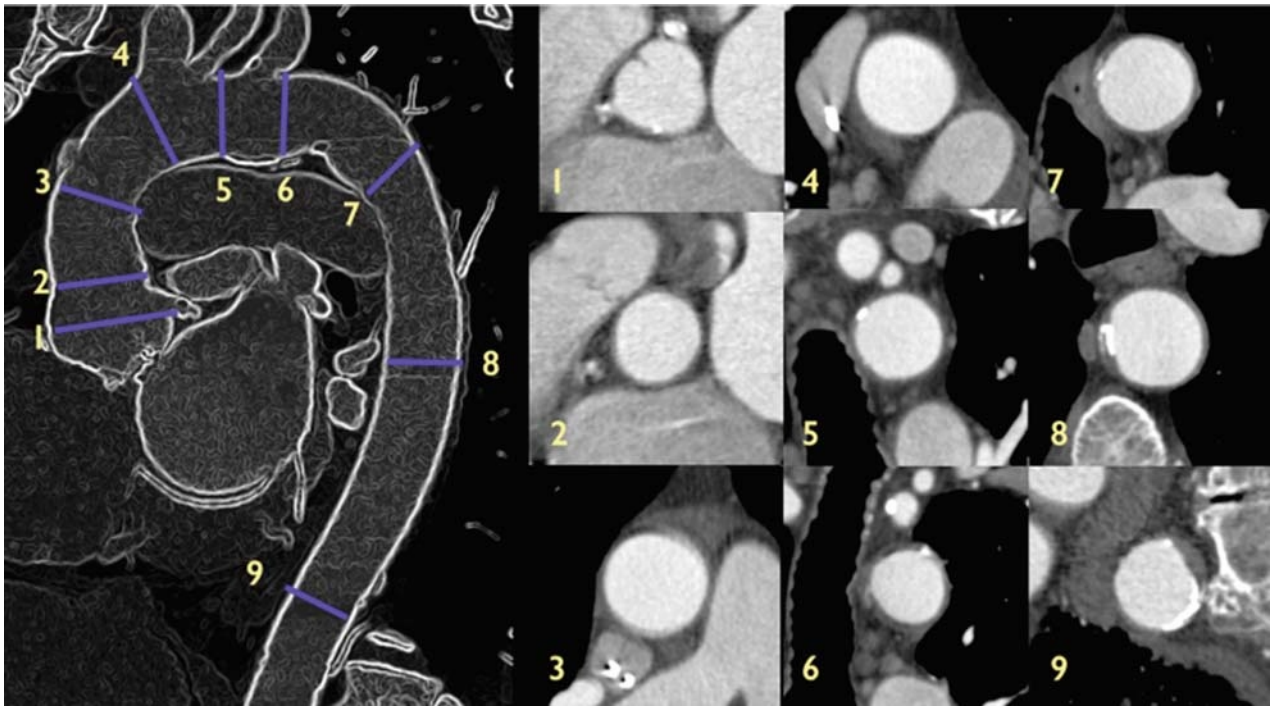

FIGURE 1. Anatomical location of measurements of the thoracic vasculature. Image (1) sinus of valsalva, (2) sinotubular junction, (3) body and (4) distal segment of the ascending aorta, (5) first segment (between innominate and left common carotid artery), (6) second segment (between the left common carotid and left subclavian artery) and (7) aortic isthmus is opposite 2 left subclavian artery where PDA is of the transverse arch, (8) proximally at the levels of the aortic valve and (9) aortic hiatus in the descending aorta. Figure 1 can be viewed online in color at www.jcat.org.

plaques of the vessel wall. When calculating the CNR, the attenuation of the right psoas muscle (ROI_{PSM}) was measured at the level of the first lumbar vertebra followed by the second measurement of noise as the standard deviation in the foam mattress of the CT table. To compare the overall degree of vascular opacification within the entire thoracic aorta, the mean opacification for each patient was measured at the mid segment of the descending thoracic aorta (ROI_{TA}). Finally, the CNR was calculated based on the measured parameters described above with an empirically derived formula:

$$CNR = (ROI_{TA} - ROI_{PSM})/Noise$$

Radiation Dose Measurement

For each of the CT scans, individual effective dose (E_{ff} [mSv]) were calculated from the dose-length products (mGy × cm), which were recorded from the patient protocol. A normalized conversion factor (k [mSv/mGy × cm]) for the chest—0.014 mSv/mGy × cm—was used to calculate the E_{ff}[19]:

$$E_{ff} = DLP \times k$$

ROC Analysis

For each protocol and scanning technique, 80 complete cases were randomly chosen with an equal number of normal (total = 40) and abnormal (total = 40) cases. Equal abnormal cases showed TAA of varying degrees as defined by 2 radiologists' reports (based on complete patient series, previous and subsequent examinations, and clinical indications). The ordering of protocol viewing was performed in a counterbalanced way: clinician 1 looked at protocol A first and then protocol B, and clinician 2 looked at protocol B first and then protocol A, and so on.

All pathology was visible on the transaxial images and the prevalence of TAA, the type of contrast administration and the scanning technique was not revealed to the observers. Technical criteria ensuring correct scan range and anatomical inclusion were considered by 2 expert cardiothoracic radiologists (not included in the study proper) to ensure that all images displayed an acceptable level of quality before they were included in the analysis.

Eight cardiothoracic radiologists who had been certified by the Royal Australian and New Zealand College of Radiologists and the American Board of Radiology respectively for a mean of 20.5 years (minimum, 13 years; maximum, 28 years) assessed

TABLE 3. Four-Point Classification Scale

	Supra-Aneurysm Filling	Partial Aneurysmal Filling	Complete Aneurysmal Filling	Infra-Aneurysmal Filling
0	1	—	—	—
1	1	1	—	—
2	1	1	1	—
3	1	1	1	1

TABLE 4. Radiation Dose: Scan Time, Scan Range and E_{ff} Between Protocols A and B

Parameters	Protocol A	Protocol B	*P*
Scan time, s	4.01 ± 1.3	4.22 ± 1.2	>0.05
Scan range, cm	55.2 ± 3.01	53.9 ± 4.03	>0.05
E_{ff} dose, mSv	3.2 ± 0.8	2.6 ± 0.4	<0.004

Data are mean ± standard deviation.

the images. All cardiothoracic radiologists were allowed to manipulate the window and level of the images during the review. Each image in the first sitting was presented and a score of 1 to 6 assigned, where 6 indicates that vascular pathology was definitely present, and 1 represented pathology definitely not present.

VGC Analysis

The VGC method of Bath and Mansson[20] was used to illustrate viewer preference of 1 technique over another based on the visibility of normal anatomy. Visual grading characteristic aims at using the fulfillment of image criteria (whether each case's image quality is fulfilled or not) and ROC (characterizing the difference between 2 protocols). Therefore, the ranking data from the cardiothoracic radiologists in a visual grading study with a multiple rating criteria is ordinal (numerical score). Specifically for this work, the presence of contrast media filling was recorded for TAA using a 4-point classification scale where score 1 indicated no contrast media filling within the TAA and 3 represented complete filling of the TAA aneurysm (Table 3).

Statistical Analysis

Measured opacity values were compared between protocols using a nonparametric Mann-Whitney *U* test. The ROC analyses employed the Dorfman-Berbaum-Metz approach using readers as random and cases as fixed.[21] Cases were treated as fixed on the basis that the limited image sample size should not be taken as representative of all images. Results were considered statistically significant if *P* is 0.05 or less.

In each scanning acquisition and contrast protocol the interobserver and intraobserver agreements were calculated using Cohen κ analysis. A *k* value of 0.60 to 1, 0.41 to 0.60, 0.21 to 0.40, and less than 0.20 was considered excellent, moderate, fair, and poor agreement, respectively.

TABLE 6. Mean Attenuation (HU) of the Descending Thoracic Aorta During TCTA

Anatomical Segment	Aneurysm Location	Protocol A	Protocol B	*P*
Descending aorta	Proximal neck	203 ± 36	420 ± 86	0.0001
	Body	190 ± 39	428 ± 88	0.0001
	Distal Neck	180 ± 32	424 ± 81	0.0001

Data are mean ± standard deviation.

RESULTS

Patient Demographics, CV, and Radiation Dose of CT Scan

There was no significant difference in sex, age, height, weight, or body mass index between the 2 protocols (all $P > 0.05$) (Table 1). Protocol A had a significantly higher CV than did protocol B (protocol A, 100 ± 1 mL; protocol B, 73 ± 10 mL; $P < 0.001$), whereas the E_{ff} dose was significantly reduced (E_{ff} was 3.2 ± 0.8 mSv for protocol A; and 2.6 ± 0.4 mSv for protocol B, $P < 0.004$). There was no significant difference in mean scan time in protocol B (4.22 ± 1.2 seconds) compared with A (4.01 ± 1.3 seconds), and scan range in each protocol (A: 55.2 ± 3.01 cm and B: 53.9 ± 4.03 cm) ($P > 0.05$) (Table 4).

Opacification of the Thoracic Aorta and Descending TAA, and CNR

Mean opacification in the thoracic aorta measured was 24% higher in protocol B (415 ± 85 HU) compared with A (325 ± 92 HU) ($P < 0.001$) (Table 5). Mean opacification in the proximal, body and distal segments of the TAA significantly increased by 55 % in protocol B compared with A (B; 424 ± 85, A; 191 ± 36 HU) ($P < 0.001$) (Table 6). In all anatomical segments and location, the mean CNR in protocol B was significantly higher than that of protocol A (B; 29.7 ± 0.61, A; 18.2 ± 12.9 HU) ($P < 0.03$) (Table 7).

TABLE 5. Mean Attenuation (HU) of Arteries at Each Anatomical Segment during TCTA

Anatomical Segment	Arterial Location	Protocol A	Protocol B	*P*
Ascending aorta	Aortic sinus	308 ± 86	416 ± 86	0.0007
	Ostia	310 ± 89	417 ± 88	0.0005
	Body	312 ± 91	418 ± 86	0.0003
	Distal	313 ± 94	416 ± 85	0.0002
Transverse aorta	First segment	311 ± 92	416 ± 84	0.0001
	Second segment	312 ± 96	415 ± 84	0.0001
	Aortic isthmus	318 ± 96	416 ± 86	0.0001
Descending aorta	Proximal	316 ± 93	411 ± 83	0.0001
	Diaphragm	316 ± 92	413 ± 81	0.0001

Data are mean ± standard deviation.

TABLE 7. Mean CNR (HU) at Each Anatomical Segment of the Thoracic Aorta

Anatomical Segment	Arterial Location	Protocol A CNR	Protocol B CNR	*P*
Ascending aorta	Aortic sinus	18.5 ± 10.3	29.7 ± 10.3	<0.03
	Ostia	19.3 ± 14.1	29.8 ± 10.1	<0.03
	Body	17.8 ± 12.2	29.9 ± 12.2	<0.02
	Distal	15.5 ± 9.4	28.7 ± 9.8	<0.03
Transverse aorta	First segment	16.6 ± 9.2	29.1 ± 11.8	<0.02
	Second segment	18.5 ± 14.0	29.4 ± 9.0	<0.03
	Aortic Isthmus	19.4 ± 14.0	29.9 ± 9.8	<0.03
Descending aorta	Proximal	18.8 ± 13.3	30.4 ± 9.3	<0.03
	Diaphragm	18.7 ± 13.1	30.7 ± 11.1	<0.03

Data are mean ± standard deviation.

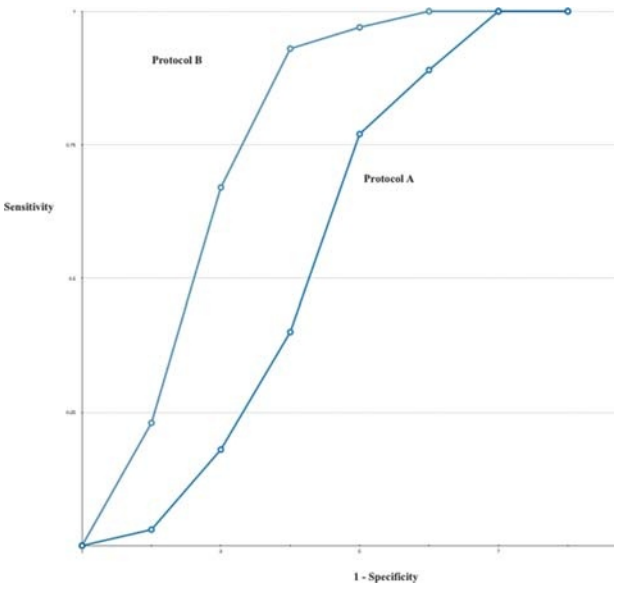

FIGURE 2. VGC curve. The circles represent the operating points corresponding to the scale steps of the rating scale. Graph represents protocol A compared with B during TCTA. Figure 2 can be viewed online in color at www.jcat.org.

Image Evaluation

Visual Grading Characteristic

The 4-point scores individually graded by the 8 readers for each TCTA protocol were expressed as a graph shown in Figure 2. When a preference is shown toward 1 protocol, the curve is convex to that protocol's axis. The graphs clearly demonstrate that when the TAA was assessed for opacification, the preference is for protocol B over A.

Receiver Operating Characteristic

The 6-point scale demonstrated a significant difference ($P < 0.005$) between protocols with mean ROC values demonstrating increased reader confidence between protocol A and B being 0.89 and 1.0, respectively (Table 8).

Kappa Analysis

Thoracic CT angiography yielded excellent interobserver agreement with protocol A ($k = 0.51$) and B ($k = 0.73$). There was a strong positive relationship between mean thoracic arterial opacification, good image quality, and reader confidence in protocol B compared with A ($r = 0.55$, $P < 0.001$).

Final Diagnosis

In protocol A, final diagnoses included significantly dilated (>6 cm) TAA (n = 32) which went on to have successful thoracic endovascular graft, and non-significant dilated (<6 cm) TAA (n = 27) and the remaining 21 patients had normal radiologic findings. In protocol B, significantly dilated TAA (n = 35) went on to have thoracic aortic endovascular graft with minor postsurgical complications, and nonsignificant dilated TAA ($n = 20$) and the remaining 25 patients had normal radiologic findings. In each regimen, both TAA which were between 4 and 6 mm are currently being monitored, and yearly TCTA scans are planned.

DISCUSSION

Intravascular opacification within the TAA during CTA examinations relies on a number of optimized parameters including contrast flow, saline bolus chase, and CV.[2,7,22] Principles of contrast protocol design are comprehensively researched in the literature; however, translating resultant complex mathematical algorithms into routine clinical practice is challenging.[14] Our study used a simple patient-specific contrast formula that included 4 key individual-specific variables obtained through routine acquisitions. The study excluded patient habitus details because linear CV based on patient size may overestimate CVs.[15,23,24]

Matching CTA acquisition with arterial opacification, it has been recommended that scan direction during CTA should be in the direction of contrast medium flow; however, with modern technology and faster scan times, change in scan direction no longer compromises vascular attenuation,[24] except when blood flow disturbances due to pathology are present. An important advantage using a caudocranial scan direction is that the exact contrast transit time at the level of the aortic hiatus can be predicted (timing bolus), irrespective of blood flow disruptions from aortic pathologies, and, therefore, maintaining peak contrast opacification throughout the entire aorta (Fig. 3). Additionally, the phenomenon of layering contrast media within aneurysms that demonstrated slow filling[25] can potentially cause interpretation errors. Therefore, caudocranial scan direction demonstrated increased arterial opacification within the thoracic aorta and TAA without contrast layering due to flow or gravity.

Using a caudocranial scan acquisition with an individualized contrast formula, it enabled significant increases in aneurysmal opacification within the thoracic aorta. Turbulent blood flow dynamics in aneurysms is still not fully understood. However, if the aneurysmal wall was rigid, the flow is pure laminar, whereas in the flexible wall of the aneurysm, a region of turbulence flow is found.[26] Our study demonstrated significant increases in contrast media filling from the proximal to the distal segment of the aneurysm with mean attenuation values in protocol B (414 ± 85 HU) compared with A (191 ± 36 HU).

Vascular opacification still remains the chief focus for all CTA protocols, and arterial attenuation above 250 HU is deemed adequate during thoracic CTA.[2,14] Our study demonstrated attenuation values above the stated threshold; however, protocol B demonstrated significantly higher mean values compared with A by 25 %. These vascular visualization changes appear to be clinically important because greater diagnostic efficacy is apparent with protocol B as evidenced by the Az values, along with improved inter-radiologist agreement.

TABLE 8. Area Under the ROC Curve for Each Observer and the Confidence Interval for TCTA Protocols

Reader	Protocol A	Protocol B
1	0.88	1.00
2	0.89	1.00
3	0.89	1.00
4	0.91	1.00
5	0.91	1.00
6	0.88	1.00
7	0.88	0.98
8	0.84	0.99
95% Confidence	0.89	1.0

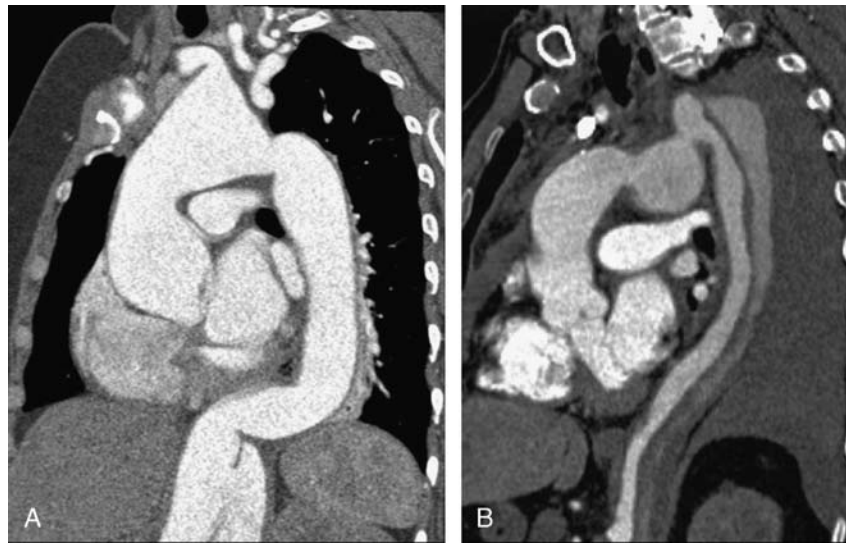

FIGURE 3. Sagittal oblique multiplanar reconstruction demonstrates two patients undergoing TCTA. Image A displays uniform arterial opacification of the thoracic aorta in a patient with multiple TAA and dissection using protocol B. Image B demonstrates poor arterial opacification of the TAA and arterial tree with protocol A.

The interplay between radiation dose and contrast protocols has often been overlooked. This is only true, when the intense contrast-filled SVC increases the radiation dose during mA modulation, thus, when the SVC is cleared from the densely filled contrast medium, this would not increase the radiation dose during CTA acquisition. Our study demonstrated mean E_{ff} in protocol B to be 2.6 mSv that is below (<8 mSv) the Internation Commission of Radiological Protection requirements for dose to the chest.[27] Additionally, with reduced CV, it significantly reduced radiation dose by 19%. With this reduction in radiation dose, there was a significant increase in CNR by 39%. Therefore, utilization of contrast media delivery at reduced CV can reduce radiation dose to patients during TCTA while increasing image quality and reader confidence.

There were shortcomings in this study. Although the results presented are promising, the use of iterative reconstruction, tube potential reduction in combination with a patient-specific contrast formula could potentially further reduce both radiation, CV, and iodine concentration during TCTA. Also, using a craniocaudal versus caudocranial scan could have been assessed separately with the use of the contrast media formula, because this could be an additional factor in reducing the delivered contrast media. Our image evaluation mainly focused on the quantitative and qualitative image criteria, whereas it did not include diagnostic accuracy of TAA in terms of sensitivity and specificity according to a reference standard.

In summary, we present a caudocranial scan acquisition and patient-specific contrast protocol that demonstrates significant improvements in visualization of thoracic aorta and aneurysm, while reducing CV, radiation dose and the potential risks of CIN during helical TCTA.

REFERENCES

1. Isselbacher EM. Trends in thoracic aortic aneurysms and dissection: out of the shadows and into the light. *Circulation*. 2014.
2. Saade C, Bourne R, Wilkinson M, et al. Caudocranial scan direction and patient-specific injection protocols optimize ECG-gated and non-gated thoracic CTA. *J Comput Assist Tomogr*. 2013;37:725–731.
3. Weiss M. Thoracic angiography using TRO-CTA—accurate diagnosis with reduced radiation dose. *Rofo*. 2013;185:417.
4. Kalmar PI, Quehenberger F, Steiner J, et al. The impact of iterative reconstruction on image quality and radiation dose in thoracic and abdominal CT. *Eur J Radiol*. 2014;83: 1416–1420.
5. Keegan J, Miglioretti DL, Gould R, et al. Radiation dose metrics in CT: assessing dose using the National Quality Forum CT patient safety measure. *J Am Coll Radiol*. 2014;11:309–315.
6. Tack D, Jahnen A, Kohler S, et al. Multidetector CT radiation dose optimisation in adults: short- and long-term effects of a clinical audit. *Eur Radiol*. 2014;24:169–175.
7. Saade C, Bourne R, Wilkinson M, et al. Contrast medium administration and parameters affecting bolus geometry in multidetector computed tomography angiography: an overview. *J Med Imag Radiat Sci*. 2011;42: 113–117.
8. Lell MM, Jost G, Korporaal JG, et al. Optimizing contrast media injection protocols in state-of-the art computed tomographic angiography. *Invest Radiol*. 2015;50:161–167.
9. Yuan R, Shuman WP, Earls JP, et al. Reduced iodine load at CT pulmonary angiography with dual-energy monochromatic imaging: comparison with standard CT pulmonary angiography—a prospective randomized trial. *Radiology*. 2012;262:290–297.
10. Engelkemier DR, Tadros A, Karimi A. Lower iodine load in routine contrast-enhanced CT: an alternative imaging strategy. *J Comput Assist Tomogr*. 2012;36:191–195.
11. Lee CH, Goo JM, Bae KT, et al. CTA contrast enhancement of the aorta and pulmonary artery: the effect of saline chase injected at two different rates in a canine experimental model. *Invest Radiol*. 2007;42: 486–490.
12. Gomes AS, Bettmann MA, Boxt LM, et al. Acute chest pain—suspected aortic dissection. American College of Radiology. ACR Appropriateness Criteria. *Radiology*. 2000;(suppl 215):1–5.
13. Nakaura T, Awai K, Yauaga Y, et al. Contrast injection protocols for coronary computed tomography angiography using a 64-detector scanner: comparison between patient weight-adjusted- and fixed iodine-dose protocols. *Invest Radiol*. 2008;43:512–519.
14. Weininger M, Barraza JM, Kemper CA, et al. Angiography: current contrast medium delivery strategies. *AJR Am J Roentgenol*. 2011;196: W260–W272.

15. Saade C, Bourne R, El-Merhi F, et al. An optimised patient-specific approach to administration of contrast agent for CT pulmonary angiography. *Eur Radiol*. 2013;23:3205–3212.
16. Lee CH, Goo JM, Lee HJ, et al. Determination of optimal timing window for pulmonary artery MDCT angiography. *AJR Am J Roentgenol*. 2007; 188:313–317.
17. Saade C, Bourne R, Wilkinson M, et al. A reduced contrast volume acquisition regimen based on cardiovascular dynamics improves visualisation of head and neck vasculature with carotid MDCT angiography. *Eur J Radiol*. 2012.
18. Melissano G, Bertoglio L, Civilini E, et al. Results of thoracic endovascular grafting in different aortic segments. *J Endovasc Ther*. 2007;14:150–157.
19. Huda W, Ogden KM, Khorasani MR. Converting dose-length product to effective dose at CT. *Radiology*. 2008;248:995–1003.
20. Bath M, Mansson LG. Visual grading characteristics (VGC) analysis: a non-parametric rank-invariant statistical method for image quality evaluation. *Br J Radiol*. 2007;80:169–176.
21. Hillis SL, Berbaum KS, Metz CE. Recent developments in the Dorfman-Berbaum-Metz procedure for multireader ROC study analysis. *Acad Radiol*. 2008;15:647–661.
22. Saade C, Wilkinson M, Parker G, et al. Multidetector computed tomography in the evaluation of cirsoid aneurysm of the scalp-a manifestation of trauma. *Clin Imaging*. 2013;37:558–560.
23. Bae KT. Optimization of contrast enhancement in thoracic MDCT. *Radiol Clin North Am*. 2010;48:9–29.
24. Saade C, Bourne R, Wilkinson M, et al. A reduced contrast volume acquisition regimen based on cardiovascular dynamics improves visualisation of head and neck vasculature with carotid MDCT angiography. *Eur J Radiol*. 2013;82:e64–e69.
25. Demehri S, Signorelli J, Kumamaru KK, et al. Volumetric quantification of type II endoleaks: an indicator for aneurysm sac growth following endovascular abdominal aortic aneurysm repair. *Radiology*. 2014;271: 282–290.
26. Lin S, Gu L. Effects of turbulent blood flow on abdominal aortic aneurysms: a fluid-structure interaction study. ASME 2013 International Mechanical Engineering Congress and Exposition, 2013. *Am Soc Mech Eng*.
27. Fujii K, Aoyama T, Yamauchi-Kawaura C, et al. Radiation dose evaluation in 64-slice CT examinations with adult and paediatric anthropomorphic phantoms. *Br J Radiol*. 2009;82:1010–1018.